

Waves in liquid films on vibrating substrates

E. S. Benilov^{1,*} and M. Chugunova^{2,†}¹*Department of Mathematics, University of Limerick, Limerick, Ireland*²*Department of Mathematics, University of Toronto, 40 St. George St., Toronto, Ontario, Canada M5S 2E4*

(Received 29 October 2009; published 1 March 2010)

This paper is concerned with liquid films on horizontally vibrating substrates. Using an equation derived by Shklyaev *et al.* [Phys. Rev. E **79**, 051603 (2009)], we show that all periodic and solitary-wave solutions of this equation are unstable regardless of their parameters. Some of the solitary waves, however, are metastable—i.e., still unstable, but with extremely small growth rates—and, thus, can persist without breaking up for a very long time. The crests of these metastable waves are flat and wide, and they all have more or less the same amplitude (determined by the problem’s global parameters). The metastable solitary waves play an important role in the evolution of films for which the state of uniform thickness is unstable. Those were simulated numerically, with two basic scenarios observed depending on the parameter $A=3(\omega/2\nu)^{1/2}U_0^2/g$, where ν is the kinematic viscosity, g is the acceleration due to gravity, and ω and U_0 are the frequency and amplitude (maximum velocity) of the substrate’s vibration. (i) If $A \lesssim 25$, a small number of metastable solitary waves with flat/wide crests emerge from the evolution and exist without coalescing (or even moving) for an extremely long time. (ii) If $A \gtrsim 25$, the solution of the initial-value problem breaks up into a set of noninteracting pulses separated by regions where the film’s thickness rapidly tends to zero.

DOI: [10.1103/PhysRevE.81.036302](https://doi.org/10.1103/PhysRevE.81.036302)

PACS number(s): 47.55.D–, 47.55.nb

I. INTRODUCTION

The effect of vibration on the stability of liquid films is of primary importance for many industrial applications. The seminal work on this problem has been done by Yih [1], who examined the linear stability of a liquid layer of uniform thickness on a substrate vibrating tangentially, i.e., in a direction in its own plane. Assuming the wavelength of the disturbance to be much larger than the liquid’s depth, Yih derived a criterion distinguishing the cases where the layer is stable from those where it is not. Then, Or [2], demonstrated that linear disturbances with wavelengths comparable to the liquid’s depth can also cause instability. The ideas of Ref. [1] were developed in a number of further papers, e.g., Refs. [3–7].

There is an important issue, however, which linear analysis cannot clarify: what happens with the film if the state of uniform thickness is unstable? Will the film evolve toward another steady state or perhaps develop some kind of chaotic motion? To answer these questions, one needs a tool for modeling the nonlinear stage of the film’s evolution—such as, for example, the lubrication approximation. Indeed, if the vibration is slow and the corresponding Reynolds number is small, one can employ the usual asymptotic approach leading to a slightly modified lubrication equation (e.g., Refs. [8–11]). If, however, the substrate’s vibration is fast, so the Reynolds number is order one, the usual lubrication approach becomes inapplicable. In this case, one needs to separate the slow film dynamics from the fast vibration-induced flow and, eventually, derive a lubrication-type equation for

the former, modified by a term describing the effect of the latter. Such an approach was used in Refs. [12,13] to study the effect of vertical vibrations on the instability of a film on a horizontal substrate.

Note, however, that vibrations that are *normal* to the substrate differ qualitatively from *tangential* vibrations: the former affect the film by changing the effective gravity and, thus, the hydrostatic pressure gradient, whereas the latter induce a sheared flow altering the film’s stability properties. Furthermore, the term in the Navier-Stokes equations describing the effect of the vibration’s vertical component is multiplied by the slope of the film’s surface, hence, under the lubrication approximation, the effect of the tangential component is much stronger (unless the vibration is close to being normal, of course).

The effect of tangential vibrations has been examined in Ref. [14], where it was shown that, if the state of uniform thickness is unstable, nonpropagating (“frozen”) periodic waves may occur on the film’s surface. In principle, these waves can be attractors, i.e., solutions originating from a wide class of initial conditions might evolve toward them. To justify such a scenario, however, one needs to ensure that the periodic waves are stable. Moreover, the problem may admit other wave solutions—such as solitary waves, for example—which could play the role of alternative attractors.

Interestingly, frozen waves generated by instabilities of vibrating liquids have been observed both experimentally [15–22] and theoretically [23–25]. These papers, however, dealt with thick liquid layers, which is different from our intended setting; furthermore, all of them except Refs. [20–22] were concerned with low-viscosity liquids.

The present paper examines the existence and stability of frozen waves developing in a thin viscous film on a vibrating substrate. Using the equation derived in Ref. [14], we show that all periodic and solitary waves that may exist on the film’s surface are unstable regardless of their parameters—but the instability of some of these solutions is so slow that

*eugene.benilov@ul.ie;

<http://www.staff.ul.ie/eugenebenilov/hpage/>

†chugunom@math.utoronto.ca;

<http://www.math.toronto.edu/chugunom/>

they should be viewed as metastable. Still, there is only one family of fully stable ‘frozen’ waves: they are similar to shock waves but with a smooth change in the film’s thickness (e.g., as in the Burgers equation). In what follows, such solutions will be referred to as “smooth-shock waves.”

The paper has the following structure: in Sec. II, the problem will be formulated and, in Secs. III–V, we shall examine the existence and stability of solitary, periodic, and smooth-shock waves, respectively. In Sec. VI, we shall simulate unstable films and, thus, elucidate which wave types emerge from the long-term evolution.

II. FORMULATION

Consider a liquid film (of density ρ , kinematic viscosity ν , surface tension σ) on a horizontal substrate vibrating tangentially with a frequency ω and amplitude (maximum velocity) U_0 .

Let h_* denote the film’s thickness, x_* denote the horizontal coordinate, and t_* the time (the asterisks indicate that the corresponding variables are dimensional). Then, the following nondimensional variables can be defined:

$$x = \left(\frac{\sigma}{\rho g}\right)^{-1/2} x_*, \quad t = \frac{\rho g^2}{\sigma \nu} \left(\frac{\nu}{2\omega}\right)^{3/2} t_*,$$

$$h = \left(\frac{\nu}{2\omega}\right)^{-1/2} h_*. \tag{1}$$

We shall assume that the slope of the film’s surface and the Reynolds number associated with the film flow are both small. The time scale of the film’s evolution is assumed to be much larger than the period of the substrate’s vibration. Under these assumptions, the film is governed by the following asymptotic equation:

$$\frac{\partial h}{\partial t} + \frac{\partial}{\partial x} \left[\frac{h^3}{3} \left(\frac{\partial^3 h}{\partial x^3} - D \frac{\partial h}{\partial x} \right) \right] = 0, \tag{2}$$

where

$$D(h) = 1 + \frac{3AF(h)}{h^3}, \tag{3}$$

and

$$F(h) = \frac{h(\cosh h \sin h + \cos h \sinh h) - 2 \sinh h \sin h}{(\cosh h + \cos h)^2}, \tag{4}$$

$$A = \frac{3U_0^2}{g} \left(\frac{\omega}{2\nu}\right)^{1/2}. \tag{5}$$

Equation (1) is a limiting case of a more general asymptotic equation derived in Ref. [14] (the latter includes an extra term describing the van der Waals attraction, which we assume weak).

The *normalized diffusivity* $D(h)$ plays an important role in the problem at hand; in particular, it determines the stability properties of a film of a uniform thickness. Indeed, seek a solution in the form

$$h = h_0 + \varepsilon h_1(x, t), \tag{6}$$

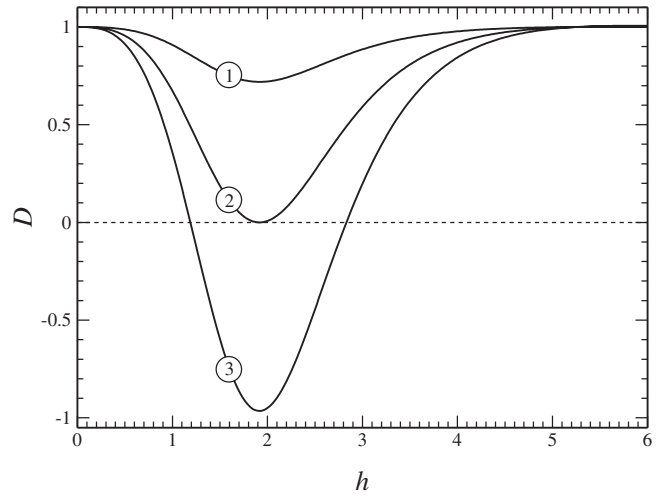


FIG. 1. The normalized diffusivity D , given by (2), vs the film’s thickness h . (1) $A=3$, (2) $A=10.688$, (3) $A=21$. Cases (1) and (2) are stable for all h ; there is an unstable region, where $D(h) < 0$, in case (3).

where h_0 is the (uniform) film’s thickness, h_1 is a disturbance, and $\varepsilon \ll 1$ is the disturbance’s amplitude. Substituting Eq. (5) into Eq. (1) and linearizing it about h_0 , we obtain

$$\frac{\partial h_1}{\partial t} + \frac{\partial}{\partial x} \left[\frac{h_0^3}{3} \left(\frac{\partial^3 h_1}{\partial x^3} - D(h_0) \frac{\partial h_1}{\partial x} \right) \right] = 0. \tag{7}$$

Consider a harmonic disturbance,

$$h_1 = e^{st} \sin kx, \tag{8}$$

where k and s are the wave number and growth/decay rate (if $s > 0$, the film is unstable). Substitution of Eq. (7) into Eq. (6) yields

$$s = -D(h_0)k^2 - k^4. \tag{9}$$

One can see that s is nonpositive (stable) for all k only if

$$D(h_0) \geq 0. \tag{10}$$

To compare the stability criterion (9), Eqs. (2)–(4) with the corresponding condition by Yih [1], observe that the two criteria coincide if the function L (introduced on page 748 of Yih’s paper) is related to “our” function F by

$$L\left(\frac{1}{2}h\right) = \frac{3F(h)}{2h^2}. \tag{11}$$

Unfortunately, Yih did not calculate L analytically (which would make the comparison straightforward), but computed it numerically. Still, “sampling” the right-hand side of Eq. (10) for various h and comparing the results with those in Yih’s Table I, one can show that Eq. (10) does hold. Note that criterion (9), Eqs. (2)–(4) has also been derived in Ref. [14], the authors of which did not realize that it had been obtained earlier.

Examples of $D(h)$ for various A are shown in Fig. 1. One can see that there is a critical value A_c such that, if $A \leq A_c$, all uniform films are stable regardless of their thicknesses. A_c can be calculated using Eq. (2),

$$A_c = \left[\max \left\{ -\frac{3F(h)}{h^3} \right\} \right]^{-1} \approx 10.688. \quad (11)$$

Note also that, despite the factor h^3 in the denominator of the second term of expression (2), $D(h)$ is regular as $h \rightarrow 0$. Indeed, the direct expansion of Eq. (3) shows that $F = O(h^6)$ as $h \rightarrow 0$, so the singularity cancels out.

III. EXISTENCE AND STABILITY OF SOLITARY WAVES

We shall seek steadily propagating waves, i.e., solutions of Eq. (1) of the form

$$h = H(x_{\text{new}}), \quad x_{\text{new}} = x - vt,$$

where v is the propagation velocity. Then, Eq. (1) yields (the subscript new omitted)

$$-vH + \frac{H^3}{3} \left[\frac{d^3H}{dx^3} - D(H) \frac{dH}{dx} \right] = c, \quad (12)$$

where c is a constant of integration. We shall require

$$H \rightarrow \bar{H} \quad \text{as} \quad x \rightarrow \pm \infty, \quad (13)$$

i.e., the solitary wave is propagating on the background of a uniform film of a thickness \bar{H} (which will be referred to as the wave's "base").

In what follows, the boundary-value problem (12) and (13) will be examined by analytical and numerical means (Secs. III A and III B, respectively). The stability of solitary waves will be examined in Sec. III C.

A. Analytical results

(i) The boundary-value problem (12) and (13) admits a solution only if $v=0$, i.e., all solitary waves in this problem are nonpropagating, or *frozen*.

Proof. Multiply Eq. (12) by $vH+c$ and rearrange it in the form

$$\frac{d}{dx} \left[(vH+c) \frac{d^2H}{dx^2} - \frac{v}{2} \left(\frac{dH}{dx} \right)^2 - G(H) \right] = \frac{3(vH+c)^2}{H^3}, \quad (14)$$

where the function $G(H)$ is such that

$$\frac{dG}{dH} = (vH+c)D(H).$$

Integrating Eq. (14) with respect to x over $(-\infty, +\infty)$ and taking into account the boundary conditions (13), we obtain

$$\int_{-\infty}^{\infty} \frac{3(vH+c)^2}{H^3} dx = 0.$$

It follows from this equality that H can be nontrivial (non-constant) only if

$$v = 0, \quad c = 0, \quad (15)$$

where the former equality proves the desired result.

Now, substitution of Eq. (15) into Eq. (12) yields a simpler equation,

$$\frac{d^3H}{dx^3} - D(H) \frac{dH}{dx} = 0. \quad (16)$$

(ii) The boundary-value problem (16) and (13) can have a solitary-wave solution only if $D(\bar{H}) > 0$. Recalling that the same requirement guarantees the stability of a film of uniform thickness \bar{H} , we conclude that solitary waves exist only on a stable base.

Proof. Taking the limit $x \rightarrow \pm \infty$ and keeping in mind that $H \rightarrow \bar{H}$, one can replace in Eq. (16) $D(H)$ with $D(\bar{H})$. The resulting linear equation can be readily solved,

$$H \rightarrow c_1 + c_2 \exp[\sqrt{D(\bar{H})}x] + c_3 \exp[-\sqrt{D(\bar{H})}x]$$

as

$$x \rightarrow \pm \infty, \quad (17)$$

where $c_{1,2,3}$ are constants. Clearly, asymptotics (17) are compatible with the boundary conditions (13) only if $D(\bar{H})$ is positive, as required.

(iii) All characteristics of a solitary wave are fully determined by the corresponding value of \bar{H} , i.e., these solutions form a single-parameter family.

Proof. Asymptotics (17) and the boundary conditions (13) imply that

$$H \rightarrow \bar{H} + c_2 \exp[\sqrt{D(\bar{H})}x] \quad \text{as} \quad x \rightarrow -\infty. \quad (18)$$

The constant c_2 can be eliminated by a suitable shift in the coordinate x , after which the above asymptotics become fully fixed. Thus, when "shooting" the solution from $-\infty$ toward $+\infty$, the only parameter that can be "prescribed" is \bar{H} , as required.

(iv) The boundary-value problem (16) and (13) admits a solution only if the normalized diffusivity D is negative for some H . As a result, solitary waves exist only in a supercritical regime, i.e., for $A > A_c$ [where A_c is determined by Eq. (11)].

Proof. Multiply Eq. (16) by dH/dx and integrate with respect to x over $(-\infty, \infty)$. Integrating by parts the third-derivative term, we obtain

$$\int_{-\infty}^{\infty} \left[\left(\frac{d^2H}{dx^2} \right)^2 + D(H) \left(\frac{dH}{dx} \right)^2 \right] dx = 0.$$

This equality shows that $D(H)$ must be negative for, at least, some values of H , as required.

Thus, even though a solitary wave's base must be stable, part of the wave's profile must be locally unstable.

B. Numerical results

In principle, Eq. (16) can be reduced to a first-order separable ODE, but the implicit solution resulting from this approach is extremely cumbersome. Much more information can be extracted from Eq. (16) numerically—and even more

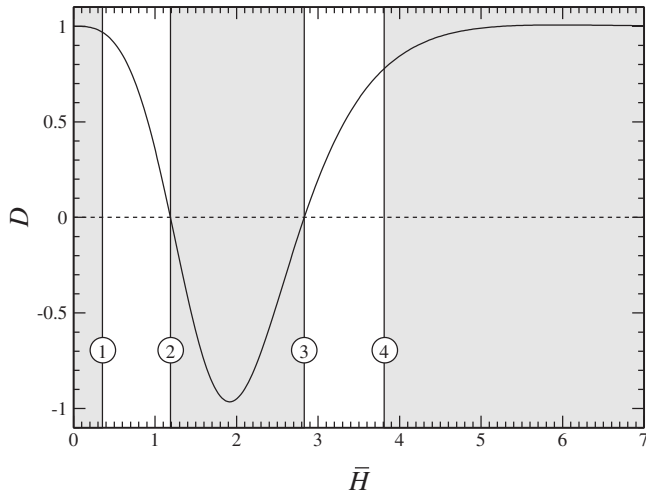


FIG. 2. The existence of solitary waves and its connection with the normalized diffusivity D , for $A=21$. \bar{H} is the wave’s base; the intervals of \bar{H} where no solutions exist are shaded. The left/right nonshaded intervals correspond to solitary waves of elevation/depression, respectively [examples shown in Figs. 3(a) and 3(b)]. Boundaries 2 and 3 correspond to the points where $D(\bar{H})$ changes sign, boundaries 1 and 2 correspond to the lower and higher critical thicknesses, \bar{H}_- and \bar{H}_+ .

so, since computing a solitary-wave solution is very simple: one just needs to set $c_2=1$ in asymptotics (18) and use it to “shoot” the solution from $-\infty$ toward $+\infty$. There are no parameters to adjust, so the solution computed is either of a solitary-wave type or not (depending, as we shall see, on the base \bar{H}).

The following conclusions were obtained.

(i) As proved in the previous section, the condition $D(\bar{H}) > 0$ is necessary for the existence of solitary waves—but our numerical results show that it is not a sufficient condition. It turns out that solitary waves exist only if their bases \bar{H} belong to one of the two intervals shown in Fig. 2. Note that boundary 2 of the left-hand interval and boundary 3 of the right-hand interval are indeed the points where $D(\bar{H})$ changes sign, but the other two boundaries do not have obvious physical interpretation. They will be discussed in more detail in Sec. V and Appendix A 2; in the meantime, they will be referred to as the *lower/higher limiting thicknesses* and denoted by \bar{H}_- and \bar{H}_+ .

(ii) Examples of solitary waves are shown in Fig. 3. Observe that, if the base \bar{H} belongs to the left-hand “existence interval” of Fig. 2, the corresponding solution is a solitary wave of *elevation*. If, on the other hand, \bar{H} belongs to the right-hand interval, the corresponding solution is a wave of *depression*. This property can be elucidated under the ap-

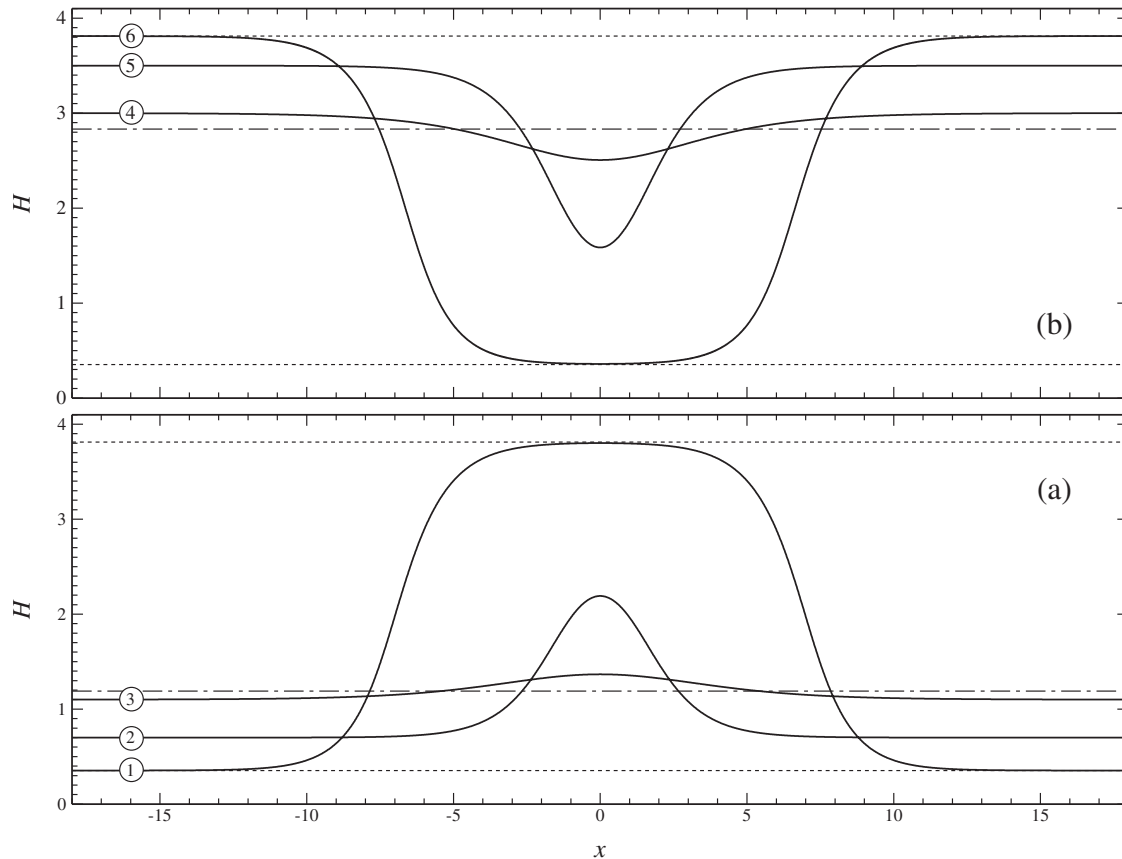


FIG. 3. Examples of solitary waves for $A=21$: (a) waves of elevation, (b) waves of depression. (1) $\bar{H}=0.35335$, (2) $\bar{H}=0.7$, (3) $\bar{H}=1.1$, (4) $\bar{H}=3$, (5) $\bar{H}=3.5$, (6) $\bar{H}=3.81158$. The dashed-dotted lines show the points where $D(\bar{H})$ changes sign [corresponding to lines (2) and (3) in Fig. 2], the dotted lines show the critical thicknesses \bar{H}_\pm [corresponding to lines (1) and (4) in Fig. 2].

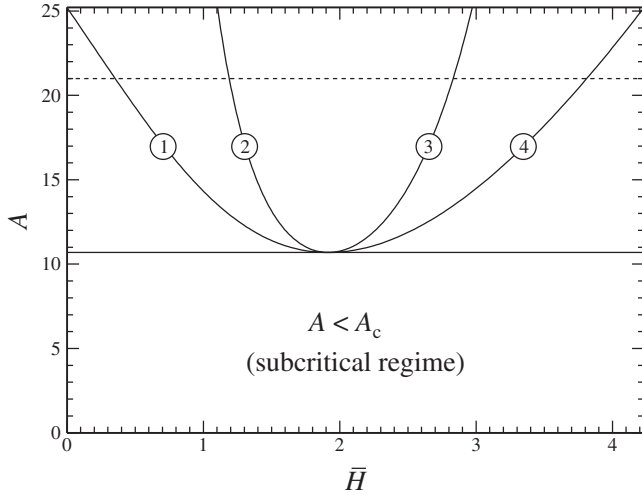


FIG. 4. The existence of solitary-wave solutions on the (\bar{H}, A) plane: solutions exist between curves 1–2 and 3–4. The dotted line shows the cross-section $A=21$ corresponding to Fig. 2.

proximation of weak nonlinearity (see Appendix A 1), which shows that the “polarity” of a solitary wave is linked to the sign of the derivative of the normalized diffusivity, $D'(\bar{H})$ (here and hereinafter, the prime ' denotes differentiation with respect to H).

(a) When \bar{H} approaches a point where $D(\bar{H})$ changes sign, the corresponding wave’s amplitude vanishes (as illustrated in Fig. 3).

(b) When the base \bar{H} of a solitary wave tends to \bar{H}_- , its amplitude tends to \bar{H}_+ [as in Fig. 3(a)] and vice versa [as in Fig. 3(b)]. In both such limits, the wave’s crest/trough becomes increasingly flat and wide. Interestingly, such solutions have been observed in nonvibrating liquids [30].

(c) The existence of solitary waves on the (\bar{H}, A) plane is illustrated in Fig. 4. One can see that, at $A=A_c$ (the critical case), both existence intervals shrink and disappear (because $D(H)$ becomes positive for all H and solitary waves cannot exist). Figure 4 shows that another important threshold exists, $A_{cc} \approx 25.209$: if $A > A_{cc}$, then \bar{H}_- is negative, which formally allows for existence of waves of elevation with negative bases and waves of depression with negative troughs. Obviously, such solutions are meaningless physically.

C. Stability of solitary waves

We shall seek a solution of the evolution Eq. (1) in the form

$$h = H(x) + h_p(x, t),$$

where H is a steady solitary wave and h_p is a small perturbation. Linearizing (1) and omitting the subscript p , one can obtain

$$\frac{\partial h}{\partial t} + \frac{\partial}{\partial x} \left[\frac{H^3}{3} \left(\frac{\partial^3 h}{\partial x^3} - D'(H)h \frac{\partial H}{\partial x} - D(H) \frac{\partial h}{\partial x} \right) \right] = 0. \quad (19)$$

We shall confine ourselves to disturbances with exponential dependence on t ,

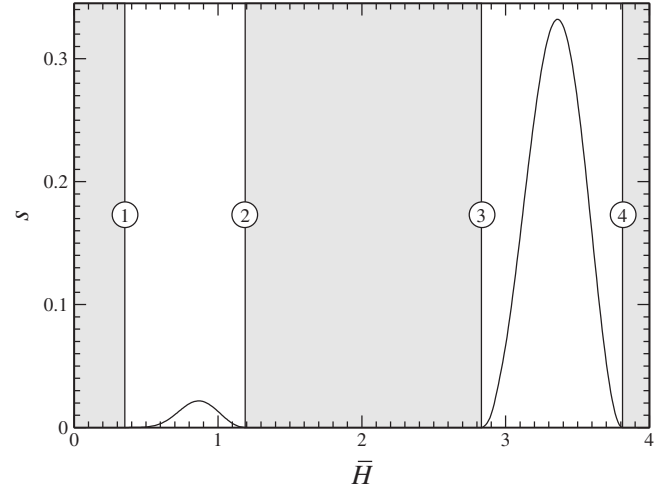


FIG. 5. The growth rate s vs a solitary wave’s base \bar{H} , for $A=21$. The regions where no solutions exist are shaded. The left/right nonshaded region corresponds to solitary waves of elevation/depression (as in Fig. 2).

$$h(x, t) = \eta(x)e^{st}, \quad (20)$$

where $\eta(x)$ describes the spatial structure of the disturbance and s is its growth/decay rate. Substituting Eq. (20) into Eq. (19), we obtain

$$-\frac{d}{dx} \left[\frac{H^3}{3} \left(\frac{d^3 \eta}{dx^3} - D'(H)\eta \frac{dH}{dx} - D(H) \frac{d\eta}{dx} \right) \right] = s\eta. \quad (21)$$

We shall require that the disturbance be localized near the solitary wave, i.e.,

$$\eta \rightarrow 0 \quad \text{as} \quad x \rightarrow \pm \infty. \quad (22)$$

Eqs. (21) and (22) form an eigenvalue problem, where $\eta(x)$ and s play the role of the eigenfunction and eigenvalue, respectively. Note also that Eq. (21) involves two parameters: the coefficient A “hidden” in expression (2) for the normalized diffusivity and the solitary wave’s base \bar{H} .

The problem (21) and (22) has been examined both analytically and numerically (in Appendix B and this section, respectively).

Analytically, it can be proved that all eigenvalues of Eq. (21) and (22) are real. Furthermore, no matter how the parameters \bar{H} and A change, the existing eigenvalues cannot change their signs. As a result, if an unstable (positive) eigenvalue exists for some values of \bar{H} and A , it exists for all values of \bar{H} and A .

Thus, to prove instability of *all* solitary waves, it is sufficient to produce a *single* example of an unstable solitary wave. This example has been obtained numerically—in fact, numerous examples have been obtained, and all solitary waves examined turned out to be unstable.

Generally, numerical results suggest that a single unstable eigenvalue exists for all values of \bar{H} and A . A typical dependence of the growth rate s on the solitary wave’s base \bar{H} is shown in Fig. 5: one can see that waves of depression are

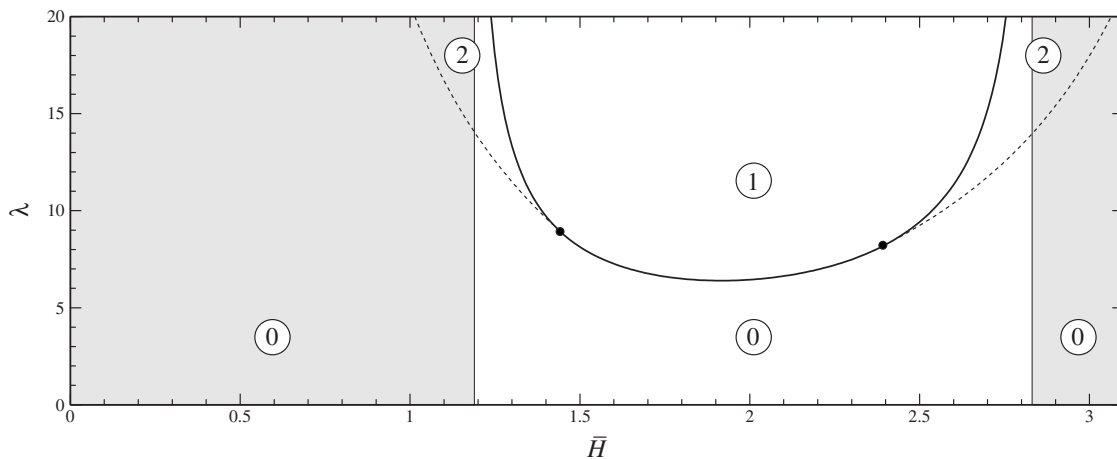


FIG. 6. The existence of periodic wave solutions depending on the mean thickness \bar{H} and period λ , for $A=21$. The circled numbers indicate how many nontrivial solutions for the same values of (\bar{H}, λ) exists in the corresponding region. The regions where the normalized diffusivity D is negative are shaded. The solid line corresponds to the linear-limit relationship (27) between \bar{H} and λ . The black dots mark the points where the dotted curves branch away from the solid one.

considerably more unstable than waves of elevation. Furthermore, the instability’s growth rate for waves with near-limiting bases, $\bar{H} \approx \bar{H}_L$, is extremely small, and these can be viewed as “metastable” states.

As shown below in Sec. VI, metastable solitary waves play a fundamental role in the general dynamics described by the evolutionary Eq. (1).

IV. EXISTENCE AND STABILITY OF PERIODIC WAVES

Periodic solutions of a generalized version of Eq. (1) (including the van der Waals effect) were examined in Ref. [14] asymptotically (in the weakly nonlinear limit) and numerically (for particular cases). The relevance of these results, however, seems to be undermined by the conclusions of Refs. [26,27], where the periodic solutions of a wide class of equations including Eq. (1) were shown to be unstable with respect to double-period perturbations.

In what follows, we shall describe the full parameter space where the periodic waves of Eq. (1) exist. We also confirm that they are unstable, and not only with respect to double-period perturbations but to *any* longer-period ones. If, however, the period of the base wave is sufficiently large, the instability’s growth rate is extremely small, and such waves can be regarded as metastable.

A. Existence of periodic waves

First of all, periodic waves of Eq. (1) are nonpropagating, or frozen (the proof of which is similar to that for solitary waves). Thus, in the absence of the propagation velocity, a periodic solution of Eq. (1) can be characterized by three parameters: the period λ , the mean thickness \bar{H} (averaged over the period), and the amplitude (i.e., the maximum deviation from the mean). It turns out, however, that these parameters are related: if any two of the three are fixed, the remaining one admits usually one or, at most, two discrete values. Accordingly, λ and \bar{H} can be treated as independent

parameters, and we shall illustrate the existence of periodic wave solutions on the (λ, \bar{H}) plane.

The steady-state Eq. (16) were solved numerically (by shooting) with the periodic boundary conditions for a wide range of parameters. The results are shown in Fig. 6. One can see that, unexpectedly, there are regions on the (λ, \bar{H}) plane where two different nontrivial (nonconstant) solutions exist for the same period and mean thickness. Examples of such solutions are shown in Fig. 7.

Some light can be shed on these multiple solutions by analyzing Eq. (16) asymptotically under an assumption of weak nonlinearity.

We shall start from an observation that, if $k = \sqrt{-D(h_0)}$, then $s=0$ —i.e., the small-amplitude solution (5), Eqs. (7) and (8) is independent of time. Thus, a small-amplitude frozen wave exists, described by

$$H(x) = H_0 + \varepsilon \sin \sqrt{-D(H_0)}x + O(\varepsilon^2), \tag{23}$$

with the period of

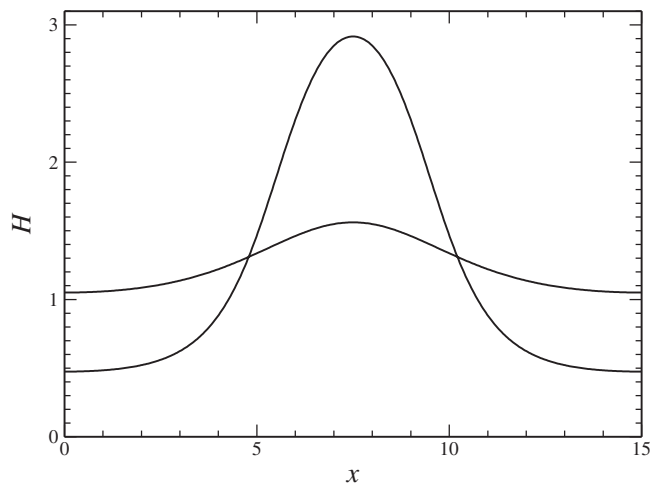


FIG. 7. An example of a pair of solutions with the same mean thickness and period, $\bar{H}=1.25$ and $\lambda=15$, for $A=21$.

$$\lambda = \frac{2\pi}{\sqrt{-D(H_0)}} \quad (24)$$

(where the capital H is used because we seek a steady-state solution). One should also keep in mind that H_0 is close, but not equal, to the film's mean thickness \bar{H} , as higher-order terms of series (23) can contribute to \bar{H} . To illustrate the difference between H_0 and \bar{H} , we calculated the next term of expansion (23), which then becomes

$$\begin{aligned} H(x) = & H_0 + \varepsilon \sin \sqrt{-D(\bar{H})}x \\ & - \varepsilon^2 \left\{ \frac{[D'(H_0)]^2 + 3D(H_0)D''(H_0)}{24D(H_0)} \right. \\ & \left. - \frac{D'(H_0)}{12D(H_0)} \cos 2kx \right\} + O(\varepsilon^3) \end{aligned} \quad (25)$$

(the derivation of this expression has been omitted, as it follows from a similar derivation carried out for the generalized version of Eq. (1) in Ref. [14]). Averaging Eq. (25) over its period, we obtain

$$\bar{H} = H_0 - \varepsilon^2 \frac{[D'(H_0)]^2 + 3D(H_0)D''(H_0)}{24D(H_0)D'(H_0)} + O(\varepsilon^3).$$

This equality can be used to express H_0 via \bar{H} ,

$$H_0 = \bar{H} + \varepsilon^2 \frac{[D'(\bar{H})]^2 + 3D(\bar{H})D''(\bar{H})}{24D(\bar{H})D'(\bar{H})} + O(\varepsilon^3),$$

then, we substitute H_0 into Eq. (24) and, thus, obtain

$$\lambda = \frac{2\pi}{\sqrt{-D(\bar{H})}} \left\{ 1 - \varepsilon^2 \frac{[D'(\bar{H})]^2 + 3D(\bar{H})D''(\bar{H})}{48D^2(\bar{H})} + O(\varepsilon^3) \right\}.$$

Observe that, depending on the sign of the expression,

$$[D'(\bar{H})]^2 + 3D(\bar{H})D''(\bar{H}), \quad (26)$$

λ may be greater or smaller than the linear-limit wavelength,

$$\lambda_{\text{lin}} = \frac{2\pi}{\sqrt{-D(\bar{H})}}. \quad (27)$$

The points where expression (26) changes sign are shown in Fig. 6 by black dots: between these, waves of small amplitude are located *above* the solid line [corresponding to the linear limit (27)]—and they are located *below* the solid line otherwise. Thus, one of the two solutions existing in the “nonuniqueness regions” of Fig. 6 can be viewed as an extension of the linear periodic wave solution, whereas the other does not have a linear limit.

Finally, the dependence of waves' shapes on their periods is illustrated in Fig. 8: one can see that, as $\lambda \rightarrow \infty$, a periodic wave's profile tends to that of a solitary wave of elevation with the limiting base \bar{H}_- (or, equivalently, a solitary wave of depression with the limiting base \bar{H}_+).

B. Stability of periodic waves

The simplest way to clarify the stability properties of periodic waves is to examine them using a suitable Lyapunov functional.

We shall start by rewriting Eq. (1) in the form

$$\frac{\partial h}{\partial t} = \frac{\partial}{\partial x} \left[\frac{h^3}{3} \frac{\partial}{\partial x} \left(D_1(h) - \frac{\partial^2 h}{\partial x^2} \right) \right], \quad (28)$$

where $D_1(h)$ is the “antiderivative” of $D(h)$, i.e.,

$$D_1(h) = \int_0^h D(\hat{h}) d\hat{h}.$$

It follows from Eq. (28) that all steady-states $h=H(x)$ satisfy

$$D_1(H) - \frac{d^2 H}{dx^2} = C, \quad (29)$$

where C is a constant of integration (this equation can also be obtained by integrating Eq. (16) with respect to x). We shall impose the condition of periodicity,

$$H(x + \lambda) = H(x), \quad (30)$$

and also require that the mean thickness assume a prescribed value \bar{H} ,

$$\frac{1}{\lambda} \int_0^\lambda H dx = \bar{H}. \quad (31)$$

Next, we introduce a functional

$$E = \frac{1}{\lambda} \int_0^\lambda \left[\frac{1}{2} \left(\frac{\partial h}{\partial x} \right)^2 + D_2(h) \right] dx, \quad (32)$$

where $h(x, t)$ is a λ periodic (but not necessarily steady) solution of Eq. (28), and $D_2(h)$ is the second “antiderivative” of $D(h)$, i.e.,

$$D_2(h) = \int_0^h D_1(\hat{h}) d\hat{h}.$$

Physically, E represents the density of energy and, given that we deal with a viscous liquid, it should not grow in time. Indeed, differentiating E with respect to t and using Eq. (28), one can readily show that, unless h is a steady state described by Eqs. (29) and (30), then

$$\frac{dE}{dt} < 0,$$

i.e., E always decreases with time. This effectively means that a steady state is stable only if it corresponds to a minimum of E —and vice versa, if there exists a disturbance reducing a steady state's energy without changing its mass, this steady state is unstable.

In what follows, we shall demonstrate that, for the family of steady-state solutions with the same mean thickness, E is a monotonically decreasing function of λ . As a result, any given periodic solution is unstable, as other solutions with the same mass exist which are close to the one given, but have a smaller energy.

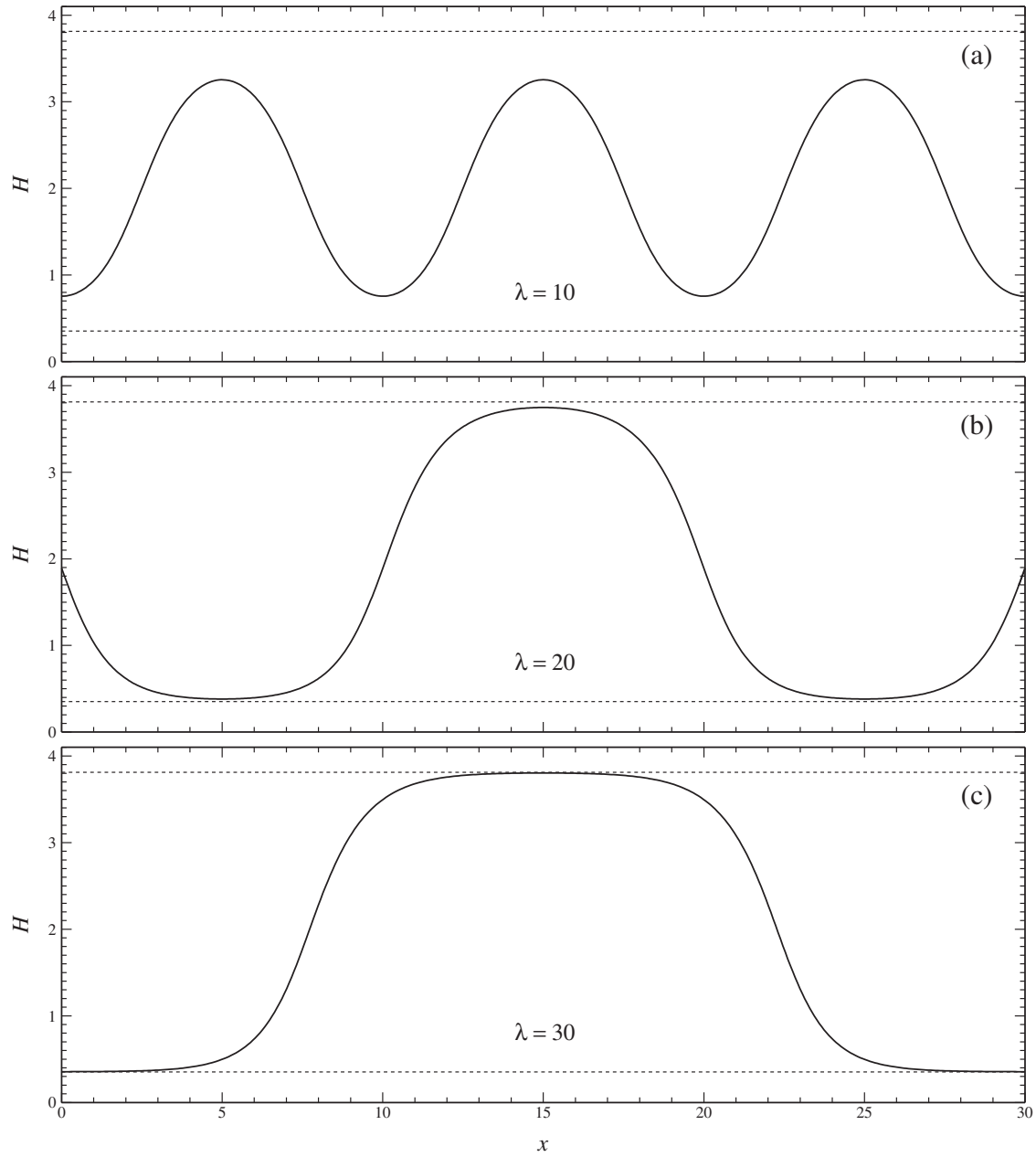


FIG. 8. The periodic wave solutions for $A=21$, $\bar{H}=2$, and $\lambda=10, 20, 30$. The dotted lines show the critical thicknesses \bar{H}_{\pm} .

To examine $E(\lambda)$, the steady-state boundary-value problem (29)–(31) can be conveniently rewritten in terms of

$$\xi = \frac{x}{\lambda},$$

which yields

$$D_1(H) - \frac{1}{\lambda^2} \frac{d^2 H}{d\xi^2} = C, \tag{33}$$

$$H(\xi + 1) = H(\xi),$$

$$\int_0^1 H d\xi = \bar{H}. \tag{34}$$

Next, substituting $h=H(\xi)$ into expression (32), rewrite it in terms of ξ ,

$$E = \int_0^1 \left[\frac{1}{2\lambda^2} \left(\frac{dH}{d\xi} \right)^2 + D_2(H) \right] d\xi.$$

Differentiating E with respect to λ , we obtain

$$E_\lambda = \int_0^1 \left[-\frac{1}{\lambda^3} \left(\frac{dH}{d\xi} \right)^2 + \frac{1}{\lambda^2} \frac{dH}{d\xi} \frac{dH_\lambda}{d\xi} + D_1(h) H_\lambda \right] d\xi,$$

where the subscript λ indicates differentiation with respect to λ . Now, integrating the second term by parts (so it would involve $d^2 H/d\xi^2$ and H_λ instead of $dH/d\xi$ and $dH_\lambda/d\xi$) and

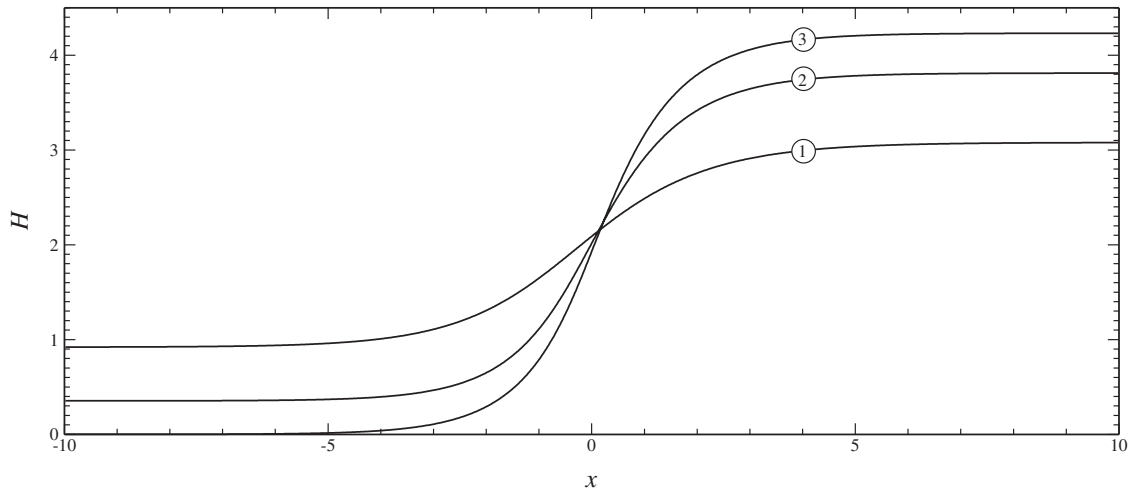


FIG. 9. The smooth-shock solutions for (1) $A=15$, (2) $A=21$, (3) $A=25.209$.

replacing $d^2H/d\xi^2$ with an appropriate expression extracted from Eq. (33), we obtain

$$E_\lambda = -\frac{1}{\lambda^3} \int_0^1 \left(\frac{dH}{d\xi} \right)^2 d\xi + C \int_0^1 H_\lambda d\xi. \quad (35)$$

Finally, differentiating Eq. (34) with respect to λ , one can see that the second term on the right-hand side of Eq. (35) is zero, hence,

$$E_\lambda = -\frac{1}{\lambda^3} \int_0^1 \left(\frac{dH}{d\xi} \right)^2 d\xi < 0$$

as required.

We comment that, not only does the above result prove that all periodic solutions are unstable, but it also predicts that the instability develops through “coarsening,” i.e., by increasing the solution’s spatial scale (as will be confirmed numerically in Sec. VI).

Finally, note that, since periodic waves with large periods are close to solitary waves with near-limiting amplitudes, one should expect the former to also be metastable.

V. EXISTENCE AND STABILITY OF SMOOTH-SHOCK WAVES

First of all, observe that solitary waves with near-limiting bases [see examples (1) and (6) in Fig. 3], as well as periodic waves with large periods [see Fig. 8(c)], can be “decomposed” into nearly uniform regions separated by regions of rapidly changing H (which will be referred to as *smooth shocks*). This suggests that a steady state exists, describing a (frozen) smooth-shock wave, such that

$$H \rightarrow \bar{H}_\pm \quad \text{as } x \rightarrow \pm \infty. \quad (36)$$

It should be emphasized that the limiting (as $x \rightarrow \pm \infty$) values of the smooth-shock solution are the same limiting thicknesses \bar{H}_\pm that came up for solitary waves. Note also that, for a given coefficient A , a unique smooth-shock solutions exists, which can be proved rigorously by analyzing the phase portrait of the steady-state Eq. (16).

Numerically, the smooth-shock solution can be found by solving Eq. (16) with the following boundary condition:

$$H \rightarrow \bar{H}_- + \exp[\sqrt{D(\bar{H}_-)}x] \quad \text{as } x \rightarrow -\infty,$$

and adjusting \bar{H}_- until the solution satisfies

$$\frac{dH}{dx} \rightarrow 0 \quad \text{as } x \rightarrow +\infty.$$

Comparing this approach with how solitary waves were computed, one would understand why the value of \bar{H}_- determined in such a way coincides with one of the two limiting thicknesses, \bar{H}_- or \bar{H}_+ .

Examples of smooth-shock waves are shown in Fig. 9. One can see that, as A increases, the jump grows and, for $A \geq 25.21$, \bar{H}_- becomes negative (such solutions are meaningless physically). Figure 10, in turn, confirms that smooth-shock solutions do describe the rapid-change regions in periodic waves with large periods and solitary waves with near-limiting bases.

With regards to stability of smooth-shock waves, it has been examined by simulating the original evolution Eq. (1). In all cases tested, these solutions turned out to be stable.

Finally, note that smooth-shock solutions have been found for liquid films in Ref. [28], and their stability has been examined in Ref. [29]. These solutions, however, have non-zero propagation speeds and, thus, are not directly relevant to the problem at hand.

VI. DIRECT SIMULATIONS OF UNSTABLE FILMS

Having examined the steady states of the evolutionary Eq. (1) and their stability, we are now able to interpret the results of numerical simulation of a “generic” initial condition and, eventually, answer the original question posed in the Introduction: what happens with a film if the corresponding state of uniform thickness is unstable?

Equation (1) was simulated using the COMSOL MULTIPHYSICS package (based on a finite-element technique). To simu-

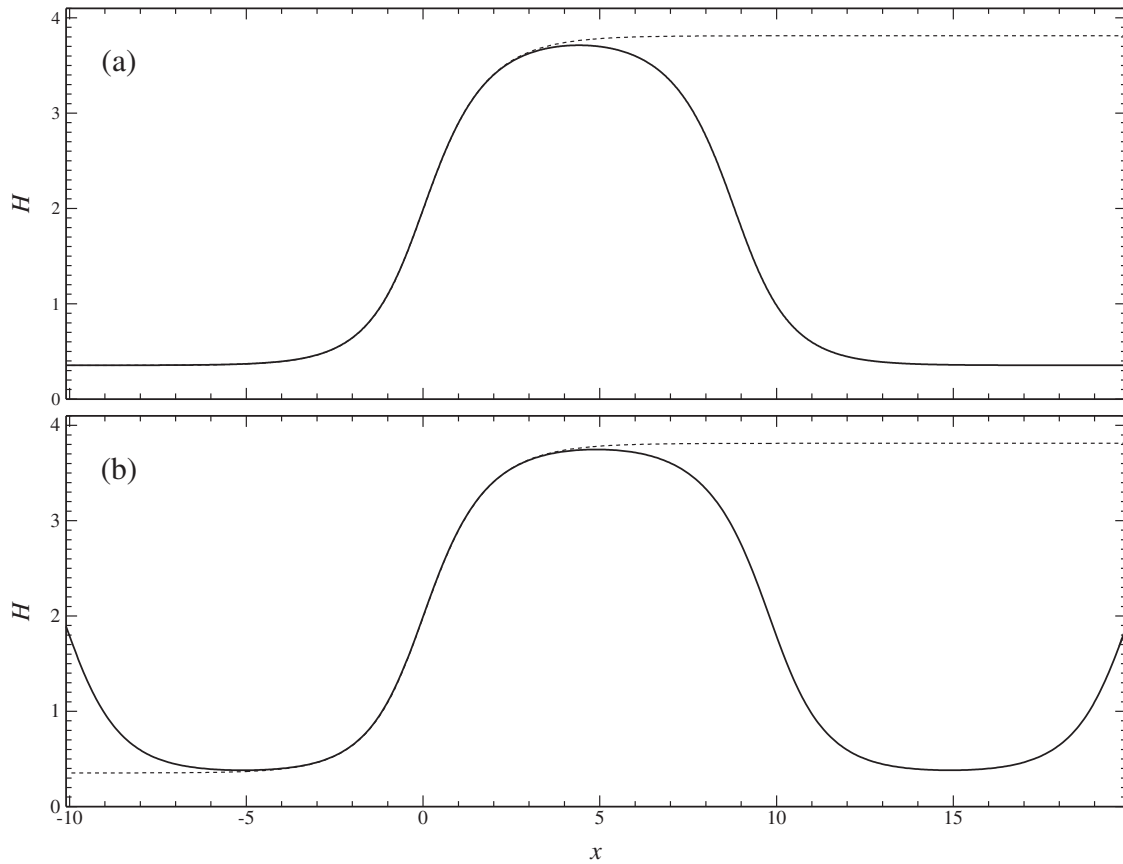


FIG. 10. A comparison of the smooth-shock wave (shown by the dotted line) with (a) solitary wave with $\bar{H}=0.3545$, and (b) periodic wave with $\bar{H}=2$, $\lambda=20$. In all cases, $A=21$.

late unbounded films, large computational domains were used, with periodic boundary conditions. A variety of initial conditions have been simulated and, in all cases where the film's mean thickness \bar{H} and the parameter A were such that $D(\bar{H}) > 0$, the solution invariably converged onto the (stable) state of uniform thickness.

In the cases where $D(\bar{H})$ was negative (hence, the state of uniform thickness was unstable), two basic scenarios were observed.

(i) If $A \leq A_{cc}$ (where $A_{cc} \approx 25.209$), the evolution can be subdivided into two stages.

(a) After a quick adjustment, the solution breaks up into a sequence of “pulses,” which may initially be periodic but gradually become irregular. With time, the pulses tend to coalesce; their amplitudes approach \bar{H}_+ , while the depths of the troughs between them tend to \bar{H}_- . Eventually, a set of solitary waves of elevation with near-limiting amplitudes and flat/wide crests is formed (the same solution can also be interpreted as a set of solitary waves of depression with flat/wide troughs). The positions and widths of the solitary waves can change quite significantly even with a slight change in the initial condition, but their crests and troughs are close to the limiting thicknesses \bar{H}_\pm and depend solely on the value of the following.

(b) Being metastable, these solitary waves can exist for an extremely long time. Further mergers may still occur, but at increasingly longer time scales.

(2) If $A \geq A_{cc}$, the solution, again, breaks up into a sequence of pulses. In contrast to the previous case, however, \bar{H}_- is formally negative, which means that the thicknesses of the regions between the pulses should (and do) tend to zero. Once these regions become sufficiently shallow, all interactions between the pulses cease and the solution no longer evolves.

Scenario 1 is illustrated in Fig. 11 for $\bar{H}=2$ and $A=21$. The size of the computational domain is $\lambda=100$. To make the solution develop faster, a small sinusoidal disturbance with near-maximum growth rate [as calculated from expression (8)] has been included in the initial condition. An even smaller long-wave disturbance, with a period equal to the size of the computation domain, has also been included (otherwise the periodic wave generated by the sinusoidal disturbance with near-maximum growth rate would persist for some time, delaying further developments). With all factors taken into account, the following initial condition was examined and presented as an illustration:

$$h = 2 + 0.02 \sin \left[\frac{11}{50} \pi (x - 10) \right] + 0.002 \sin \left[\frac{1}{50} \pi (x - 10) \right], \quad (37)$$

where the first sine represents the disturbance with a near-maximum growth rate, the second sine represents the long-wave disturbance, and the -10 shift has been added to make

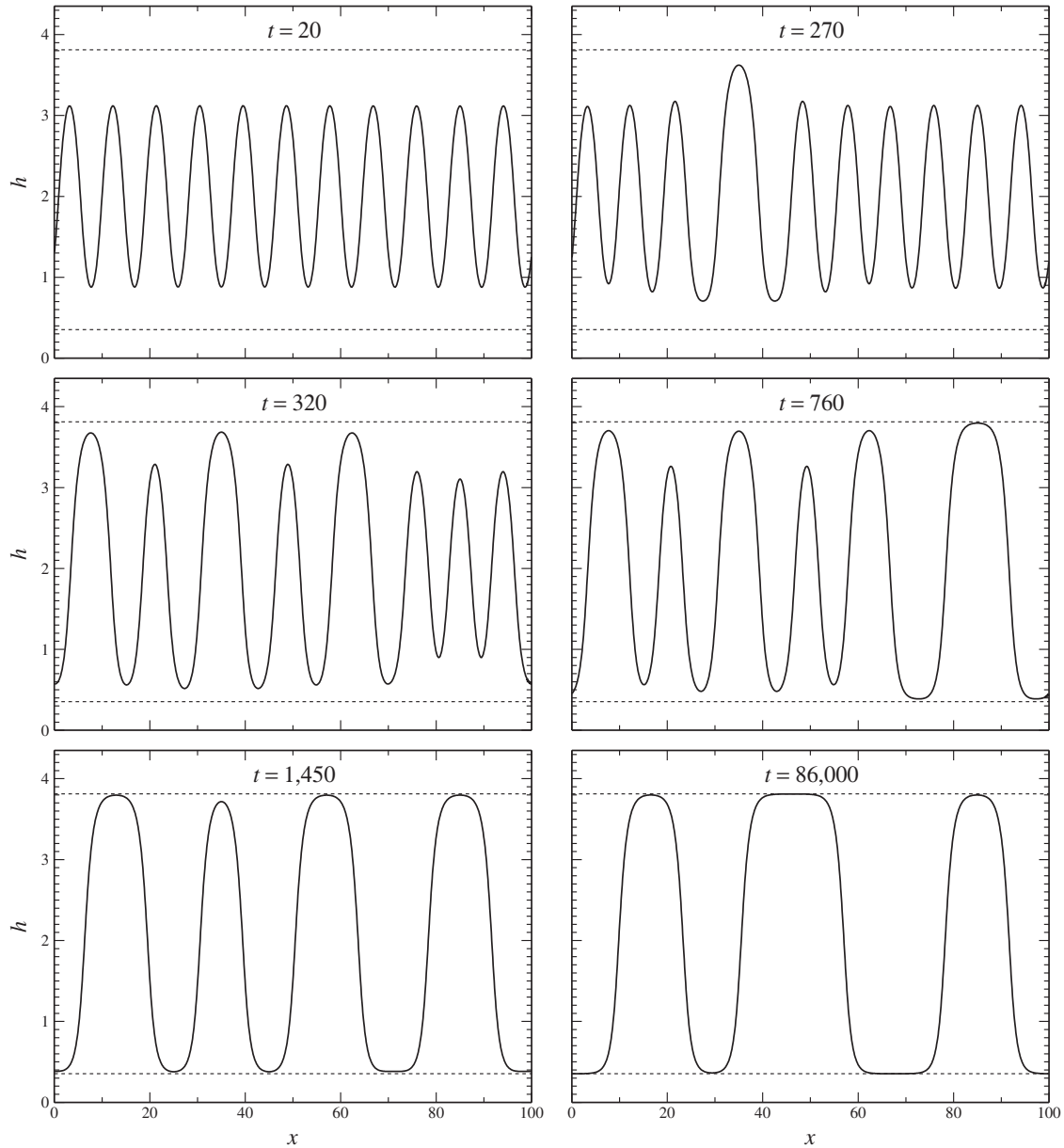


FIG. 11. The solution of the initial-value problem (1) and (37) for $A=21$.

the large- t solution better “visible” in Fig. 11.

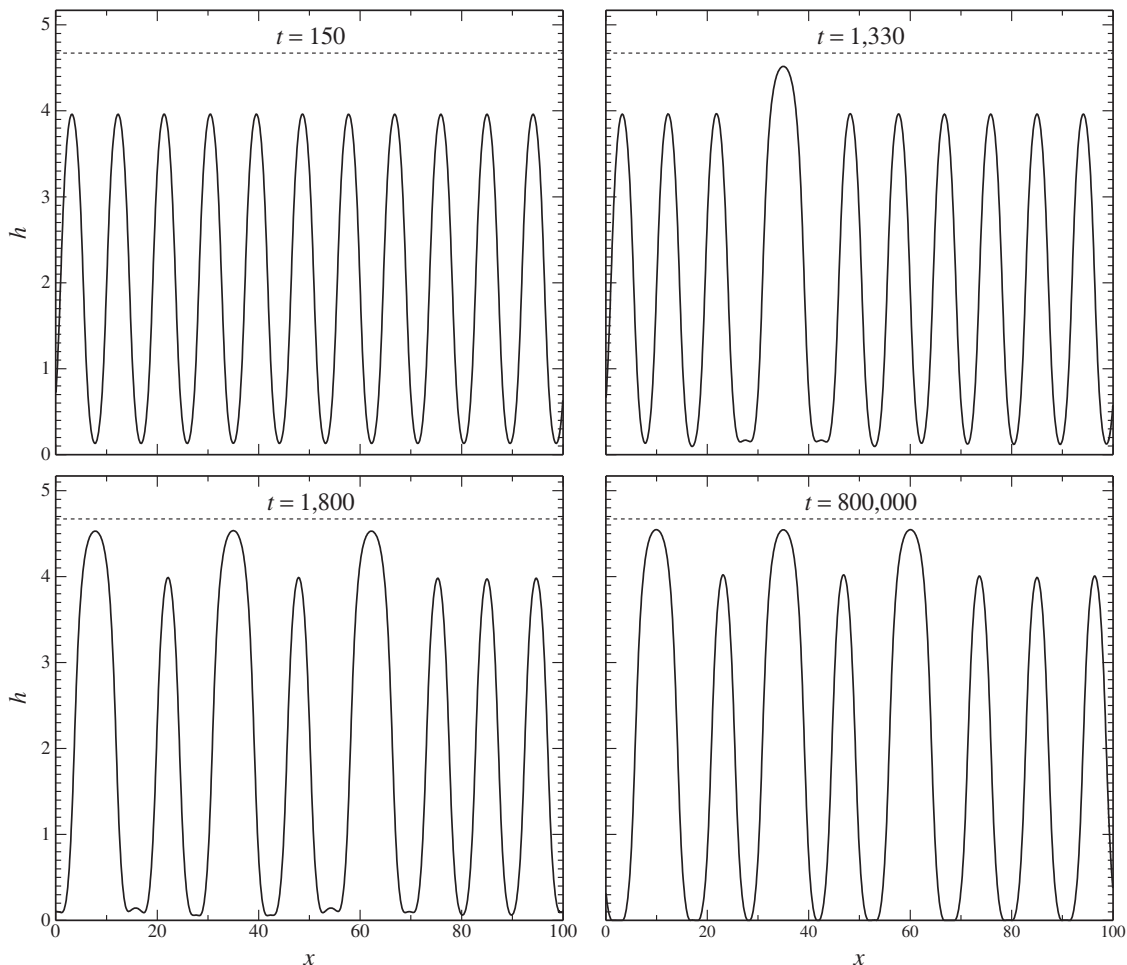
Initially, the disturbance with near-maximum growth rate rapidly grows, but at $t \sim 20$, it saturates (see Fig. 11) and a periodic wave is formed. During $t \sim 250-270$, two crests of the wave coalesce, then (during $t \sim 300-320$) another two mergers occur simultaneously. Further mergers follow until only three peaks are left at $t \sim 86,000$, after which the solution becomes metastable (at least, we were unable to run the simulation long enough to reach another merger).

Scenario 2 is illustrated in Fig. 12 for $A=30$ (the rest of the parameters and the initial condition are the same as before). This time, only three mergers occur during the whole simulation, then, the troughs between the pulses become shallow and, thus, weaken the pulses’ interactions. After the last merger, no changes occur in the pulses’ shapes or amplitudes, although some of the pulses might change slightly their positions. In Fig. 12, for example, the first and third of

the three larger pulses shift a little bit, which can be observed by carefully comparing the “snapshots” at $t=1,800$ and $t=800,000$. This simulation ran until $t=1,200,000$, but no further sizable shifting occurred. Note also that the pulses do not get anywhere close to the limiting amplitude.

VII. SUMMARY AND CONCLUDING REMARKS

Thus, we have examined liquid films on vibrating substrates using the model Eq. (1) derived previously in Ref. [14]. Three types of nonpropagating (frozen) solutions—solitary, periodic, and smooth-shock waves—have been examined, and only the last type turned out to be fully stable. Some of the solitary and periodic waves, however, are metastable and, thus, can persist without breaking up for an extremely long time. The crests of metastable solitary waves are flat and wide, while their bases and amplitudes depend

FIG. 12. The solution of the initial-value problem (1) and (37) for $A=30$.

solely on the parameter A given by expression (4). Metastable periodic solutions have similar properties, plus their periods must be large.

Metastable solitary waves play an important role in the evolution of films for which the state of uniform thickness is unstable. Two different scenarios have been observed.

(i) If $A \lesssim 25$, a small number of solitary waves with flat/wide crests emerge from the evolution. They are metastable and, thus, exist without coalescing (or even moving) for an extremely long time.

(ii) If $A \gtrsim 25$, the solution of the initial-value problem breaks up into a set of noninteracting pulses separated by regions where the film's thickness rapidly tends to zero (reflecting the fact that, for $A \gtrsim 25$, the bases of the metastable solitary waves are, formally, negative).

In conclusion, we shall briefly discuss how the present results can be extended to more realistic models.

First, Eq. (1) can be readily generalized to include evaporation, which would be particularly important if $A \gtrsim 25$. Indeed, in such cases, evaporation can cause the developing thin-film regions to completely dry up.

Second, Eq. (1) can be extended to substrates inclined at an angle α ,

$$\frac{\partial h}{\partial t} + \frac{\partial}{\partial x} \left[\frac{h^3}{3} \left(\frac{\partial^3 h}{\partial x^3} - D \frac{\partial h}{\partial x} + \sin \alpha \right) \right] = 0, \quad (38)$$

with a modified expression for the normalized diffusivity,

$$D(h) = \cos \alpha + \frac{3AF(h)}{h^3}, \quad (39)$$

where $F(h)$ is given by Eq. (3). It can be demonstrated that the wave solutions of Eq. (38) are no longer frozen but propagate down the slope. Observe also that, with growing α , the interval for which $D(h)$ is negative expands (see Fig. 13)—as a result, the range of thicknesses where uniform films are unstable broadens.

Third, Eq. (1) can be generalized for nonharmonic (generally periodic or random) vibrations of the substrate. In this case our nondimensional variables need to be modified, as they involve the frequency of the substrate's vibration (which is no longer a well-defined quantity). In fact, the simplest option here is to use the original dimensional variables, in terms of which the governing equation is

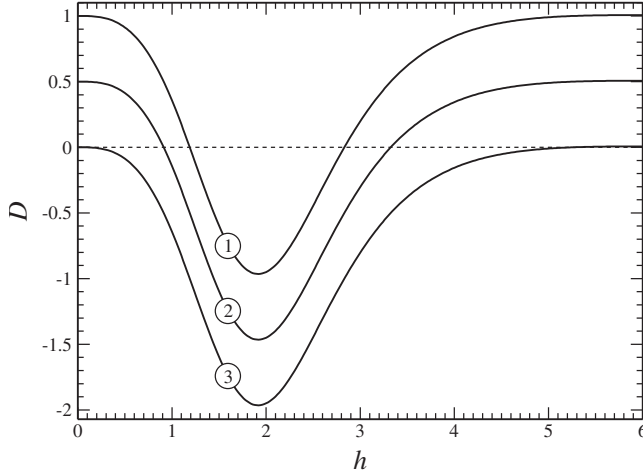


FIG. 13. The normalized diffusivity (39) and (3) for a sloping substrate, for various angles of inclination: (1) $\alpha=0^\circ$, (2) $\alpha=60^\circ$, (3) $\alpha=90^\circ$.

$$\frac{\partial h_*}{\partial t_*} + \frac{g}{\nu} \frac{\partial}{\partial x_*} \left[\frac{h_*^3}{3} \left(\frac{\sigma}{\rho g} \frac{\partial^3 h_*}{\partial x_*^3} - D \frac{\partial h_*}{\partial x_*} + \sin \alpha \right) \right] = 0, \quad (40)$$

where the normalized diffusivity is given by

$$D(h_*) = \cos \alpha + \frac{9\nu}{gh_*^3} \int_0^\infty \frac{A(\omega)}{\omega^3} F \left(\sqrt{\frac{2\omega}{\nu}} h_* \right) d\omega, \quad (41)$$

and $\hat{A}(\omega)$ is the Fourier transform of the second moment of the substrate's tangential acceleration $a(t)$,

$$A(\omega) = \frac{1}{2\pi} \int_{-\infty}^{\infty} \langle a(t)a(t+\tau) \rangle e^{-i\omega\tau} d\omega, \quad (42)$$

where the angle brackets imply time averaging. Equation (40) can be derived in a similar fashion to how the original Eq. (1) was derived in Ref. [14].

It can be verified that the case of harmonic vibration can be recovered from Eqs. (40)–(42) by assuming that $a(t) = U_0 \omega_0 \sin \omega_0 t$, hence,

$$A(\omega) = \frac{1}{4} U_0^2 \omega_0^2 [\delta(\omega - \omega_0) + \delta(\omega + \omega_0)],$$

where $\delta(\omega)$ is the Dirac delta function.

ACKNOWLEDGMENTS

The authors acknowledge the support of the Science Foundation Ireland, delivered via RFP Grant under Grant No. 08/RFP/MTH1476 and Mathematics Initiative Grant under Grant No. 06/MI/005.

APPENDIX A: WEAKLY NONLINEAR SOLITARY WAVES

We shall seek a solitary-wave solution of Eq. (16) in the form

$$H(x) = \bar{H} + \tilde{H}(x),$$

where \bar{H} is the wave's base. Assuming that the wave's amplitude is small, i.e., $|\tilde{H}| \ll \bar{H}$, we can expand $D(H)$ in Eq. (16) and thus obtain

$$\frac{d^3 \tilde{H}}{dx^3} - \left[D(\bar{H}) + D'(\bar{H})\tilde{H} + \frac{1}{2} D''(\bar{H})\tilde{H}^2 + \dots \right] \frac{d\tilde{H}}{dx} = 0, \quad (A1)$$

where $' = d/dh$. We shall also formulate the boundary conditions (13) in terms of \tilde{H} ,

$$\tilde{H} \rightarrow 0 \quad \text{as} \quad x \rightarrow \pm \infty. \quad (A2)$$

1. General case

Note that if $D(\bar{H})$ is order one, the second and further terms in the square brackets in Eq. (A1) should be omitted, resulting a linear equation which does not have solitary-wave solutions. Thus, we need to retain at least one nonlinear term, which implies that \bar{H} must be chosen in such a way that

$$|D(\bar{H})| \ll 1,$$

i.e., \bar{H} is close to one of the roots of $D(H)$ —see Fig. 14(a). In this case, we can keep the first and second terms of the expansion of $D(H)$ in Eq. (A1) and, thus, obtain

$$\frac{d^3 \tilde{H}}{dx^3} - [D(\bar{H}) + D'(\bar{H})\tilde{H}] \frac{d\tilde{H}}{dx} = 0. \quad (A3)$$

Integrating Eq. (A3) and using conditions (A2) to eliminate the constant of integration, we obtain

$$\frac{d^2 \tilde{H}}{dx^2} - D(\bar{H})\tilde{H} - \frac{1}{2} D'(\bar{H})\tilde{H}^2 = 0.$$

This ODE is well-known in the context of the Korteweg-de Vries equation (of which it is a steady-wave reduction). For the boundary conditions (A2), it has a unique solitary-wave solution,

$$\tilde{H} = -\frac{3D(\bar{H})}{D'(\bar{H})} \operatorname{sech}^2 \left(\frac{\sqrt{D(\bar{H})}}{2} x \right). \quad (A4)$$

Observe the following.

(i) As expected, solution (A4) is physically meaningful only if $D(\bar{H}) > 0$, i.e., its base must be stable.

(ii) If $D'(\bar{H}) < 0$, solution (A4) describes a wave of elevation, whereas $D'(\bar{H}) > 0$ corresponds to a wave of depression.

(iii) Solution (A4) is fully determined by its base \bar{H} , i.e., it represents a single-parameter family of solutions.

2. Limit of weak supercriticality

One can see that solution (A4) becomes singular in the limit $D'(\bar{H}) \rightarrow 0$, which violates our original assumption of weak nonlinearity.

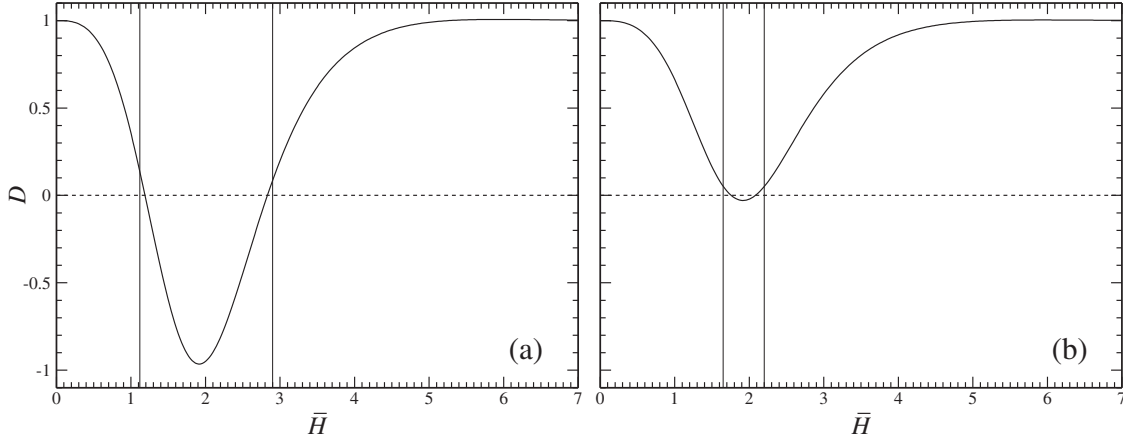


FIG. 14. The normalized diffusivity D as a function of a solitary wave's base \bar{H} for (a) $A=21$, (b) $A=11$. The vertical lines show examples of \bar{H} allowable for weakly nonlinear waves [\bar{H} should be located in an area where $1 \gg D(\bar{H}) > 0$]. Observe that, in case (b), weak nonlinearity implies that $|D'(\bar{H})| \ll 1$.

To remedy this inconsistency, we shall return to Eq. (A1) and take into account an extra term in the expansion of $D(H)$, which yields

$$\frac{d^3 \tilde{H}}{dx^3} - \left[D(\bar{H}) + D'(\bar{H})\tilde{H} + \frac{1}{2}D''(\bar{H})\tilde{H}^2 \right] \frac{d\tilde{H}}{dx} = 0. \quad (\text{A5})$$

Observe that keeping all three terms in the square brackets implies that

$$|D(\bar{H})| \ll 1, \quad |D'(\bar{H})| \ll 1$$

[see Fig. 14(b)]. It can be shown that these conditions can hold simultaneously only in the case of weak supercriticality, i.e., when A is slightly larger than

$$A_c \approx 10.688,$$

while \bar{H} is close to

$$H_c \approx 1.916,$$

where H_c is the value of H where $D(H)$ has a minimum for $A=A_c$.

Equation (A5) can be integrated with respect to x , then multiplied by $d\tilde{H}/dx$ and integrated again, which yields

$$\frac{1}{2} \left(\frac{d\tilde{H}}{dx} \right)^2 - \left[\frac{D(\bar{H})}{2} \tilde{H}^2 + \frac{D'(\bar{H})}{6} \tilde{H}^3 + \frac{D''(\bar{H})}{24} \tilde{H}^4 \right] = b_1 \tilde{H} + b_2, \quad (\text{A6})$$

where $b_{1,2}$ are the constants of integration. It can be shown that the solution of Eq. (A6) satisfies the boundary conditions (A2) only if $b_{1,2}=0$, after which Eq. (A6) becomes

$$\left(\frac{d\tilde{H}}{dx} \right)^2 = D(\bar{H})\tilde{H}^2 + \frac{1}{3}D'(\bar{H})\tilde{H}^3 + \frac{1}{12}D''(\bar{H})\tilde{H}^4.$$

To find the solitary wave's amplitude \tilde{H}_a , one needs to equate the right-hand side of this equation to zero, which yields

$$\tilde{H}_a = \frac{-2D'(\bar{H}) \pm 2\sqrt{[D'(\bar{H})]^2 - 3D(\bar{H})D''(\bar{H})}}{D''(\bar{H})}. \quad (\text{A7})$$

Note that the assumption of weak supercriticality (under which the above formula was obtained) implies that the normalized diffusivity can be approximated by

$$D(H) \approx \frac{A_c - A}{A_c} + \frac{1}{2}\beta(H - H_c)^2, \quad (\text{A8})$$

where

$$\beta = [D''(H_c)]_{A=A_c} \approx 2.165$$

[formula (A8) can be extracted from the general expression (2) under the assumptions $A \approx A_c$, $H \approx H_c$]. Substituting Eq. (A8) into Eq. (A7), we obtain

$$\tilde{H}_a = -2(\bar{H} - H_c) \pm \sqrt{3(\beta A_c)^{-1}(A - A_c) - \frac{1}{2}(\bar{H} - H_c)^2}.$$

It can be readily verified that \tilde{H}_a is real only if $\bar{H}_- \leq \bar{H} \leq \bar{H}_+$, where

$$\bar{H}_{\pm} = H_c \pm \sqrt{6(\beta A_c)^{-1}(A - A_c)}. \quad (\text{A9})$$

These expressions approximate the limiting thicknesses for the weakly supercritical regime (if plotted in Fig. 4, dependencies Eq. (A9) would approximate curves 1 and 4 as $\bar{H} \rightarrow H_c$).

APPENDIX B: THE PROPERTIES OF THE EIGENVALUE PROBLEM (21) and (22)

Note, that the operator on the left-hand side of Eq. (20) is not self-adjoint, which complicates the problem. To bypass the difficulty, we shall introduce $\phi(x)$, such that

$$\eta = \frac{d\phi}{dx}, \quad (\text{B1})$$

$$\phi \rightarrow 0 \quad \text{as} \quad x \rightarrow -\infty. \quad (\text{B2})$$

Then, Eq. (21) yields

$$-\frac{d^4\phi}{dx^4} + \frac{d}{dx} \left[D(H) \frac{d\phi}{dx} \right] = \frac{3s}{H^3} \phi. \quad (\text{B3})$$

Next, it follows from Eqs. (21) and (22) that

$$\int_{-\infty}^{\infty} \eta dx = 0$$

and, together with Eqs. (B1) and (B2), this equality implies that

$$\phi \rightarrow 0 \quad \text{as} \quad x \rightarrow \pm\infty. \quad (\text{B4})$$

In the remainder of this section, we shall examine the properties of the eigenvalue problem (B3) and (B4).

(i) It can be verified by inspection that:

(a) the eigenvalue problem (B3) and (B4) admits the following solution:

$$s = 0, \quad \phi = H.$$

(b) It can be further shown (by analyzing Eq. (B3) with $s=0$) that the above is the *only* solution with $s=0$.

(ii) Since the operator on the left-hand side of Eq. (B3) is self-adjoint, and the weight function $3/H^3$ on the right-hand side is positive, then

(a) the eigenvalue problem (B3) and (B4) can have only real eigenvalues.

(b) Any two eigenfunctions, ϕ_1 and ϕ_2 , such that $s_1 \neq s_2$, satisfy the condition

$$\int_{-\infty}^{\infty} \frac{\phi_1 \phi_2}{H^3} dx = 0. \quad (\text{B5})$$

Properties 2(a) and 2(b) can be proved by multiplying Eq. (B3) by an appropriate function [e.g., the complex conjugate of ϕ for Property 2(a)] and integrating with respect to x over $(-\infty, \infty)$. Most importantly, it follows from Property 2(b) that, if two eigenvalues coalesce due to a change in parameters \bar{H} or A , the corresponding eigenfunctions must remain different (otherwise, the integral on the left-hand side of Eq. (B5) would not be zero). Together with Property 1(b), this means that changes in \bar{H} or A cannot make an initially non-zero eigenvalue s coalesce with $s=0$. Finally, taking into account Property 2(a), we conclude that, if a positive (unstable) eigenvalue exists for some \bar{H} and A , it can never become stable, as it is “trapped” on the positive part of the real axis.

Thus, to show instability of *all* solitary waves, it is sufficient to show instability of *one* solitary wave.

-
- [1] C. S. Yih, *J. Fluid Mech.* **31**, 737 (1968).
 [2] A. C. Or, *J. Fluid Mech.* **335**, 213 (1997).
 [3] S. P. Lin, J. N. Chen, and D. R. Woods, *Phys. Fluids* **8**, 3247 (1996).
 [4] A. C. Or and R. E. Kelly, *J. Fluid Mech.* **360**, 21 (1998).
 [5] M. R. King, D. T. Leighton, and M. J. McCready, *Phys. Fluids* **11**, 833 (1999).
 [6] P. Gao and X.-Y. Lu, *J. Fluid Mech.* **562**, 345 (2006).
 [7] M. G. Blyth, *J. Eng. Math.* **59**, 123 (2007).
 [8] A. Oron and O. Gottlieb, *Phys. Fluids* **14**, 2622 (2002).
 [9] O. Gottlieb and A. Oron, *Int. J. Bifurcation Chaos Appl. Sci. Eng.* **14**, 4117 (2004).
 [10] L. Moldavsky, M. Fichman, and A. Oron, *Phys. Rev. E* **76**, 045301(R) (2007).
 [11] A. Oron, O. Gottlieb, and E. Novbari, *Eur. J. Mech. B/Fluids* **28**, 37 (2009).
 [12] U. Thiele, J. M. Vega, and E. Knobloch, *J. Fluid Mech.* **546**, 61 (2005).
 [13] S. Shklyaev, M. Khenner, and A. A. Alabuzhev, *Phys. Rev. E* **77**, 036320 (2008).
 [14] S. Shklyaev, A. A. Alabuzhev, and M. Khenner, *Phys. Rev. E* **79**, 051603 (2009).
 [15] G. H. Wolf, *Z. Phys.* **227**, 291 (1969).
 [16] W. González-Viñas and J. Salán, *EPL* **26**, 665 (1994).
 [17] R. Wunenburger, P. Evesque, C. Chabot, Y. Garrabos, S. Fauve, and D. Beysens, *Phys. Rev. E* **59**, 5440 (1999).
 [18] A. A. Ivanova, V. G. Kozlov, and P. Evesque, *Fluid Dyn.* **36**, 362 (2001).
 [19] M. Legendre, P. Petitjeans, and P. Kurowski, *C. R. Mec.* **331**, 617 (2003).
 [20] E. Talib, S. V. Jalikop, and A. Juel, *J. Fluid Mech.* **584**, 45 (2007).
 [21] E. Talib and A. Juel, *Phys. Fluids* **19**, 092102 (2007).
 [22] S. V. Jalikop and A. Juel, *J. Fluid Mech.* **640**, 131 (2009).
 [23] D. V. Lyubimov and A. A. Cherepanov, *Fluid Dyn.* **21**, 849 (1986).
 [24] M. Khenner and D. Lyubimov, *Hydrodynamika* **11**, 191 (1998) (in Russian).
 [25] M. V. Khenner, D. V. Lyubimov, T. S. Belozerovalova, and B. Roux, *Eur. J. Mech. B/Fluids* **18**, 1085 (1999).
 [26] R. S. Laugesen and M. C. Pugh, *Arch. Ration. Mech. Anal.* **154**, 3 (2000).
 [27] R. S. Laugesen and M. C. Pugh, *J. Differ. Equations* **182**, 377 (2002).
 [28] A. L. Bertozzi and M. Shearer, *SIAM J. Math. Anal.* **32**, 194 (2000).
 [29] A. L. Bertozzi, A. Munch, M. Shearer, and K. Zumbrun, *Eur. J. Appl. Math.* **12**, 253 (2001).
 [30] D. V. Lyubimov and S. V. Shklyaev, *Fluid Dyn.* **37**, 545 (2002).